Telomeric damage in early stage of chronic lymphocytic leukemia correlates with shelterin dysregulation

*Adeline Augereau,[1,2] *Claire T'kint de Roodenbeke,[1] Thomas Simonet,[1] Serge Bauwens,[1] Béatrice Horard,[1] Mary Callanan,[3,4] Dominique Leroux,[3,4] Laurent Jallades,[5] Gilles Salles,[6] Eric Gilson,[1,2,7,8] and Delphine Poncet[1-7]

[1]Epigenetic and Telomeric Regulations, Lyon Sud Medicine Faculty, Lyon-1 University, Centre National de la Recherche Scientifique (CNRS) Unité Mixte de Recherche (UMR) 5239, Pierre Bénite, France; [2]Laboratory of Biology and Pathology of Genomes, University of Nice, Medicine Faculty, UMR 6267 CNRS U998 Inserm, Nice, France; [3]Inserm, U823, Institut Albert Bonniot, Grenoble, France; [4]Université Joseph Fourier-Grenoble I, Grenoble, France; [5]Laboratoire d'Hématologie, Hospices Civils de Lyon, Centre Hospitalier Lyon Sud, Pierre Bénite, France; [6]Hospices Civils de Lyon, Lyon-1 University, CNRS UMR 5239, Pierre Bénite, France; [7]Hospices Civils de Lyon, Centre Hospitalier Lyon Sud, Unité Médicale d'Oncologie Moléculaire et Transfert, Service de Biochimie, Pierre Bénite, France; and [8]Department of Medical Genetics, Centre Hospitalier Universitaire (CHU) de Nice, Archet 2 Hospital, Nice, France

Cells of B-cell chronic lymphocytic leukemia (B-CLL) are characterized by short telomeres despite a low proliferative index. Because telomere length has been reported to be a valuable prognosis criteria, there is a great interest in a deep understanding of the origin and consequences of telomere dysfunction in this pathology. Cases of chromosome fusion involving extremely short telomeres have been reported at advanced stage. In the present study, we address the question of the existence of early telomere dysfunction during the B-CLL time course. In a series restricted to 23 newly diagnosed Binet stage A CLL patients compared with 12 healthy donors, we found a significant increase in recruitment of DNA-damage factors to telomeres showing telomere dysfunction in the early stage of the disease. Remarkably, the presence of dysfunctional telomeres did not correlate with telomere shortening or chromatin marks deregulation but with a down-regulation of 2 shelterin genes: *ACD* (coding for TPP1; *P* = .0464) and *TINF2* (coding for TIN2; *P* = .0177). We propose that telomeric deprotection in the early step of CLL is not merely the consequence of telomere shortening but also of shelterin alteration. (*Blood*. 2011; 118(5):1316-1322)

Introduction

Telomere erosion in proliferating cells leads to senescence[1] and is thereby a potent barrier for tumor progression.[2] In normal proliferating cells, such as germ and stem cells and in cancer cells, this erosion is compensated mainly by a specialized reverse transcriptase named telomerase.[3,4] This enzyme is crucial in cancer cells for tumor progression.[5] However, telomere shortening because of telomerase invalidation can also cooperate with p53 deficiency to facilitate carcinogenesis in aged mice.[6] In chronic lymphocytic leukemia (CLL), despite a low proliferative index, telomeres are abnormally shortened[7] and we previously reported a low telomerase expression level.[8] In this context, both the consequence and the origins of telomere shortening are still a matter of debate.[9] This point is of great importance as telomere shortening has been shown to be an even better prognosis marker than the reference one, namely the mutational status of *IGHV* gene.[10] In this way, recent publications reported the presence of deprotected telomeres in radio-resistant patient cells[11] and fused telomeres bearing extremely short telomeres in patients mainly at advances stages of the disease.[12] Both of these studies proposed that telomere dysfunction or crisis can be at the origin of genomic instability and karyotype abnormality accumulation observed during disease progression.

A priori, the telomere injuries observed in CLL could stem from an excessive telomere shortening or alteration in the protective chromatin structure that cap telomeres or both. Indeed, if maintenance of telomere length depends on telomerase,[13] telomere protection involves various telomere-associated proteins, such as the shelterin complex[1] composed of 6 proteins (TRF1, TRF2, RAP1, TIN2, TPP1, POT1)[14] (Figure 1). This complex appears to act as a hub that protects telomeres from being recognized as a double-strand break, thereby avoiding inappropriate DNA damage response (DDR) activation and aberrant repair[15] (Figure 1). This complex also controls telomere length, by regulating both the telomerase activity[16-19] and the alternative lengthening of telomere (ALT) mechanism.[20] These proteins are also involved in oncogenesis. For instance, TRF2 is up-regulated in various types of human tumors[21] and has been found to display oncogenic properties in mouse keratinocytes[22] and human cancer cell lines.[23] Human telomeres are also composed of nucleosomes that exhibit repressive chromatin marks, such as H3K9 and H4K20 trimethylation and low histone acetylation level[24] associated to a hypermethylation of CpG in the subtelomeric regions. In agreement with a role for these chromatin modifications in telomere length control, the invalidation of enzymes responsible for their formation, that is, histone methyltransferase such as Suv39h1, Suv39h2, Suv4-20h, or DNA methyl transferase as DMNT1, 3a and 3b, leads to changes in telomere size.[25-27]

We have previously shown a global deregulation of the expression of shelterin proteins in an heterogeneous cohort of CLL patients.[8] Here, we address the question of whether telomere dysfunction occurs at early stages of CLL and, if yes, whether it can

Submitted July 9, 2010; accepted February 6, 2011. Prepublished online as *Blood* First Edition paper, February 25, 2011; DOI 10.1182/blood-2010-07-295774.

*A.A. and C.T.d.R. contributed equally to this study.

This article is a continuation of a previous report.[8]

The publication costs of this article were defrayed in part by page charge payment. Therefore, and solely to indicate this fact, this article is hereby marked "advertisement" in accordance with 18 USC section 1734.

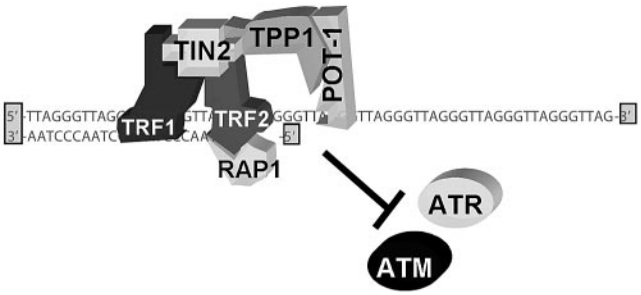

Figure 1. The shelterin complex. Telomere DNA extremity is schematized at the junction between double strand DNA an 3′ single-strand overhang. The shelterin complex is composed of 2 double-strand telomeric sequence–binding proteins (TRF1 and TRF2), of one 3′overhang-binding protein (POT1) and of 3 others proteins (TIN2, TPP1, RAP1), essential for the complex constitution and stabilization. This complex inhibits DDR activation and ATM and/or ATR activation.

be correlated with telomere shortening and/or changes in the telomere chromatin cap. As an early sign of telomere dysfunction, we monitored the recruitment at telomeres of DDR proteins. Thus, we restricted our analysis to B cells from 23 patients of first stage of CLL leukemogenesis (Binet stage A, < 2 years of disease history, previously untreated). We used B cells from 12 healthy age-matched donors as control.

We found a significant increase in telomeric damage in CLL patients in comparison with healthy donors. Strikingly, the presence of dysfunctional telomere at this early stage of the disease did not correlate with short telomeres but rather with a down-regulation of 2 shelterin genes: *ACD* and *TINF2*. We thus propose that early telomere deprotection in CLL results from shelterin dysregulation rather than from telomere shortening.

Methods

Patients and healthy donors

After informed consent and according to institutional guidelines, total blood samples were collected from 23 CLL patients at the Hospices Civils de Lyon and Grenoble University and from 12 age-matched healthy donors at the Etablissement Français du Sang. The protocol has been approved by the institutional review board. The diagnosis was based on morphologic criteria and immunophenotyping (Matutes score > 3/5). Patients were newly diagnosed (< 2 years of disease history) stage A patients, not previously treated by chemotherapy. Disease stage, FISH data, and *IGH* mutational

Table 1. Sample characteristics

				FISH analysis				Available datas			
Sample	Disease stage	Mutational status	Karyotype	17p13	11q23	del13q14	+12	CHIP	IF	qPCR	Teloblot
CLL											
ALD	A	M	A	N	N	t + del m	N	√	√	√	√
ARM	A	M	N	N	N	N	N	√	√	√	√
BAR	A	UM	ND	del	N	N	N	√	ND	√	√
BRI	A	M	N	N	N	N	N	√	√	√	√
CAR	A	M	ND	N	N	del m	N	√	ND	√	√
Dan37	A	M	N	N	N	del m	N	√	√	√	√
Dan39	A	M	N	N	N	del m	N	√	√	√	ND
DUR	A	M	ND	N	N	del m + b	N	√	√	√	√
ECH	A	M	ND	N	N	del m	N	√	√	√	√
FRA	A	UM	ND	N	N	N	N	√	ND	√	√
GUI	A	M	N	N	N	N	N	ND	ND	ND	ND
IRE	A	UM	A	N	del	del m	N	√	ND	ND	√
JOS	A	UM	N	N	del	N	N	√	√	√	√
JOU	A	M	ND	N	N	del m + b	N	ND	√	ND	ND
LOU	A	M	N	N	N	N	N	√	√	√	√
LUC	A	M	A (complex)	N	N	N	N	√	√	√	√
MAR	A	M	ND	N	N	del b	N	√	√	√	√
MAR38	A	M	A (+12)	N	N	N	+12	√	√	√	√
MAR6	A	M	N	N	N	del m + b	N	√	√	√	√
PIE	A	M	N	N	N	del m + b	N	√	√	√	√
RIC	A	M	N	N	N	N	N	√	√	√	√
SOL	A	UM	N	N	N	del m	N	√	√	√	√
SUZ	A	M	N	N	N	del m	N	√	√	√	√
Co											
N120	NA	NA	NA	NA	NA	NA	NA	√	√	ND	√
N121	NA	NA	NA	NA	NA	NA	NA	√	√	√	√
N122	NA	NA	NA	NA	NA	NA	NA	√	√	ND	√
N123	NA	NA	NA	NA	NA	NA	NA	√	√	ND	√
N124	NA	NA	NA	NA	NA	NA	NA	√	√	√	√
N125	NA	NA	NA	NA	NA	NA	NA	√	√	√	√
N126	NA	NA	NA	NA	NA	NA	NA	√	√	√	√
N127	NA	NA	NA	NA	NA	NA	NA	√	ND	ND	√
N128	NA	NA	NA	NA	NA	NA	NA	√	√	√	√
N129	NA	NA	NA	NA	NA	NA	NA	√	√	ND	√
N132	NA	NA	NA	NA	NA	NA	NA	√	√	√	√
N133	NA	NA	NA	NA	NA	NA	NA	√	√	ND	√

NA indicates nonapplicable; ND, not done; M, mutated; UM, unmutated; A, abnormal; N, normal; del, deletion; m, monoallelic; b, biallelic; del, deletion; +12, trisomy 12; and t, translocation.

status are provided for each patient in Table 1. Briefly, del13q, del11q, del17p, and t12 were, respectively, found in 56%, 8,7%, 4%, and 4% of patients and 22% of patients are unmutated. These percentages for some are inferior to what is found in general CLL patients,[28] are in accordance with those observed in stage A patients.[29,30]

Isolation of human B cells

B lymphocytes were purified from peripheral blood by using the human CD19 Microbeads kit (Miltenyi Biotec). Briefly, Ficoll prepared PBMCs were incubated with a cocktail of anti-CD19 antibody-conjugated magnetic microbeads. The magnetically labeled CD19-positive cells are collected by passing over a MACS column in a magnetic MACS separator. Cells were washed 3 times, eluted from the column and tested for CD19 enrichment. Percentage of CD19-positive cells was determined by flow cytometry (LSRII; BD Biosciences Pharmingen) using an α-CD19–PE antibody (Amersham Pharmacia Biotech). Over 93% of CD19-positive labeling was obtained for normal B cells and CLL cells. For CHIP experiments only, patient blood samples showing $>80\%$ B-CLL cells were not further purified after Ficoll gradient separation.

Immunofluorescence

Cells were fixed in cold methanol (−20°C), washed twice in PBS, incubated 40 minutes in 1× Target Retrieval Solution (DAKO) at 95°C, cooled 20 minutes at room temperature, and rinsed 3 times in distilled water. Slides were then incubated 1 hour in blocking solution (50mM NaCl, 0.5% Triton X-100, 3% dry skimmed milk in PBS) and immunostained overnight at 37°C by 1:300 rabbit anti-53BP1 (NB 100-305; Novus Biologicals) and mouse anti-TRF1 (ab10579; Abcam) in blocking solution. After 3 rinses in 0.8%, PBS, 1.5% dry skimmed milk, 50% NaCl, slides were incubated 1 hour in blocking solution containing Alexa Fluor 555–conjugated anti–mouse (A-31 570; Molecular Probes/Interchim) and Alexa Fluor 488 anti–rabbit (A-21 206; Molecular Probes) antibodies at 37°C. Slides were mounted in VectaShield antifade reagent (Vector Laboratories/CliniSciences) and observed thanks to a confucal microscope (Axioplan2 LSM510, Carl Zeiss) with plan achromal 63×/1.4 oil objective and the Zeiss LSM510 v3.2 acquistion software. Optical sections were recorded at room temperature with a z-step <200 nm to determine the occurrence of 53BP1/TRF1 colocalizations, at least 30 nuclei per condition were analyzed.

Chromatin immunoprecipitation

Formaldehyde-fixed cells (0.75%) were washed and lysed. After nuclei membrane lysis, chromatin was recovered and sonicated on BioRuptor Sonicator (Diagenode). Chromatin (about 800-bp fragments) was separated in different fractions (corresponding to 2.5 million cells for the IgG and 1 million cells for the input and each histone directed antibody used), and precleared (premixed protein A and G sepharose 4 Fast-Flow 50%/50%; Amersham). Fractions were incubated overnight at 4°C with 5 μg of anti H3K9 trimetlyated (07-442; Milipore), H3K9 acetylated (07-352; Milipore), total H3 (ab1791; Abcam), or 10 μg of irrelevant mouse immunoglobulin (I8765; Sigma-Aldrich). After 1 hour of incubation premixed beads were washed 4 times in buffer of increase stringency. Eluates were, subjected to RNAse A treatment (1 hour, 37°C, 1 mg of RNAse A; Roche), reverse cross-linked (65°C, overnight in 20mM NaCl). Protein digestion was done at 45°C for 1 hour with 20 mg of Proteinase K (Roche). DNA was purified (classic phenol/chloroform method) before being spotted thanks to Bio-Dot SF system (Bio-Rad). Ten percent of DNA precipitated was spotted on a Hybon N+ membrane (GE Healthcare). DIG-labeled (DIG-High Prime kit; Roche Applied Bioscience) telomeric (400 bp of repeated 5′-T_2AG_3-3′ motif) or ALU (173 bp of genomic DNA amplified using primers 5′-TGAAACCCCGTCTCTACTAAAA-3′ and 5′-GTCTCGCTCT-GTCGCCCA-3′). (Plasmids are available on request to E.G. or B.H.) Probes were used for membrane hybridization. Chemiluminescent signals were scanned with a CDD camera image analyzer system (LAS-300; Fujifilm). Bands were quantified by Image J software. Signals were quantified thanks to a linear regression obtained by plotting the signal (arbitrary units) in function of the percentage of input.

Southern blot determination of telomere size (Teloblot)

Telomere size was determined by terminal repeat fragment (TRF) experiments, considering the maximal intensity peak by using Image J software. Briefly, genomic DNA was purified following the DNeasy blood and Tissue kit (QIAGEN) instructions. Four micrograms of DNA was digested overnight by 4 μL of *Hin*fI and 4 μL of *Rsa*I (New England Biolabs). After precipitation, DNA was diluted in 1× TE (Tris 10mM, EDTA 1mM) and subjected to 1% low-melting agarose (Bio-Rad) gel electrophoresis for 15 hours in Chef Mapper DRIII (Bio-Rad) at 3.5 V/cm^2. DNA was blotted to N+ Hybond membrane (GE Healthcare) by capillarity transfer in SCC 20× buffer and then UV cross-linked. Hybridization and detection of the telomeric sequences were performed as for ChIP experiments.

RT and Q-PCR

RNA was extracted from 5 million purified B cells using the TRIzol reagent according to the manufacturer's instructions (Invitrogen) and reverse transcribed using the high-capacity cDNA reverse transcription kit (Applied Biosystems). Custom-made 384-well TaqMan Low Density Arrays (TLDA) were used for quantitative PCR (Q-PCR) amplification with the TaqMan Gene expression master mix on a 7900HT Fast Real-Time PCR system (Applied Biosystems). The geometrical mean of 5 references genes was used for gene expression normalization. References genes (*HDAC3, MBD4, WRN, DKC1, ATR*) were selected by geNorm software (http://medgen.ugent.be/~jvdesomp/genorm/) with a pairwise variation (V) inferior to 0.15.

Statistical analyses

Considering the sample size, we performed nonparametric 2-sample Wilcoxon rank-sum tests (also called the Mann-Whitney *U* test), using R software to test significance of mean differences in each experiment.

Results

Study design

We performed our experiments on B lymphocytes purified from the peripheral blood of 12 healthy donors and 23 newly diagnosed and previously untreated stage A CLL patients coming from 2 different hospitals. The patients fulfilled the classic CLL phenotypic and molecular criteria (Table 1 and see "Patients and healthy donors"). As expected,[31,32] the CLL patients exhibited an increased BCL2 expression and decreased Ki67 expression, known to be responsible for a higher antiapoptotic activity in a low proliferating rate context (Figure 2A). Importantly, this cohort of patients harbors the previously published features of telomere changes, that is, a general decrease in telomere length ($P = .0025$) in CLL lymphocytes compared with normal B cells and an even shorter length in *IGVH* unmutated versus mutated patients ($P = .0015$; Figure 2B). Therefore, we are studying a representative panel of mutated and unmutated patients as far as classic CLL markers and telomere length are concerned.

Telomere dysfunction in early stages of CLL oncogenesis

Recent studies[8,10,33-35] have reported telomeric damage[11,12] and imbalances of shelterin protein expression in CLL,[8] but no study has as yet addressed the question of the origin of telomere damage in these patients. To determine whether CLL telomeres are deprotected and thereby recognized as DNA damages, we performed double immunofluorescence analyses: interphasic cells were immunostained with antibodies against TRF1 (a marker of telomeres) and 53BP1 (a DDR factor). The data were analyzed by

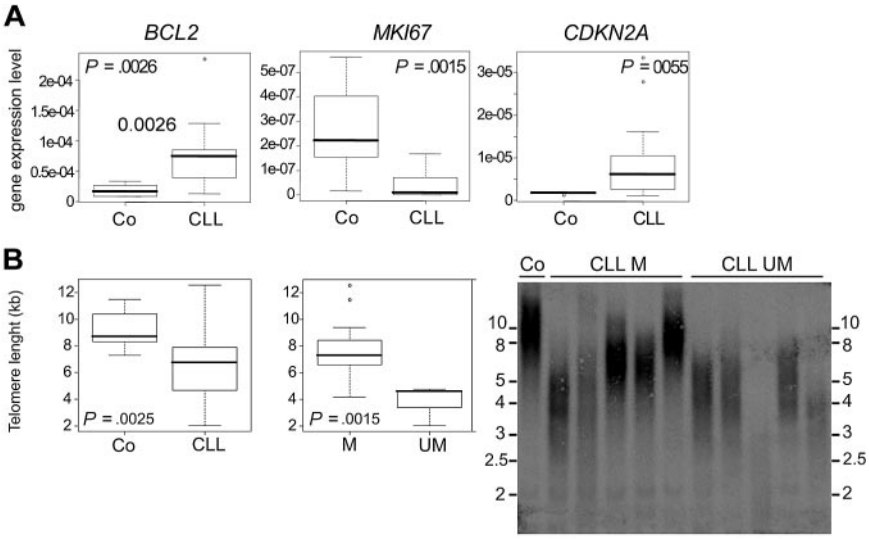

Figure 2. CLL classic molecular and telomeric features. (A) *BCL2*, *MKI67*, and *CDKN2A* (respectively coding for Bcl2, Ki67, and p16) normalized gene expression level, quantified in purified B cells from 6 healthy donors and 20 stage A CLL patients. Wilcoxon test *P* values are indicated in each corresponding box plot. (B) Telomeric size was analyzed by Teloblotting on B lymphocytes purified from 12 healthy donors and 20 CLL patients. Box plot showing telomere size, with corresponding Wilcoxon test calculated *P* values in healthy (Co) versus CLL (CLL) B cells (left) and in mutated (M) versus unmutated (UM) CLL B cells (right). A representative picture of telomeric restriction fragment analysis of one normal B cells (Co), 5 CLL mutated patients (CL M), and 5 CLL unmutated patients (CLL UM) is shown (right). Telomere size (in kb) was calculated thanks to specific ladder, size is indicated on each side of the Teloblot.

confocal microscopy to score the number of 53BP1 foci colocalizing with telomeres forming the so-called TIFs (telomere dysfunction–induced foci[36]). In our experimental conditions, we only rarely detected the presence of 53BP1 foci in B cells from healthy donors (median of 0.03 focus per nucleus; Figure 3B-C). However, in CLL we found a significant 6-fold increase in 53BP1-positive foci (median of 0.18 focus per nucleus, $P = .0485$). As a comparison, we found a 17-fold increase in 53BP1 foci after 5Gy γ irradiation in one of the patients (Figure 3A). We observed an even more statistically relevant increase in TIF in CLL versus healthy donors (median of 0.08 vs 0 TIF per nucleus, $P = .02352$; Figure 3B-C). Thus, TIF represent roughly 44% of 53BP1 foci in B-CLL cells, thereby indicating that a significant proportion of DNA damage is linked to telomere dysfunction in CLL. In agreement with these median values, we were unable to detect TIF in 63% (7/11) of healthy and 22% (4/18) of CLL cells, allowing us to classify healthy and CLL donors in subgroups named TIF$^+$ (presence of TIF) and TIF$^-$ (absence of TIF).

These data confirm a previous study showing the presence of TIF in CLL cells[11] and further show that TIF occur during early stage of CLL. It is worth noting that the increase of TIF in CLL might have been underestimated because very short telomeres might not lead to detectable TRF1-positive foci.

Telomere deprotection in CLL patients does not correlate with mean telomere length

Because CLL cells have shorter telomeres than normal B cells, we asked whether the increased frequency of TIF in CLL patients is because of an excessive telomere shortening. Strikingly, whereas

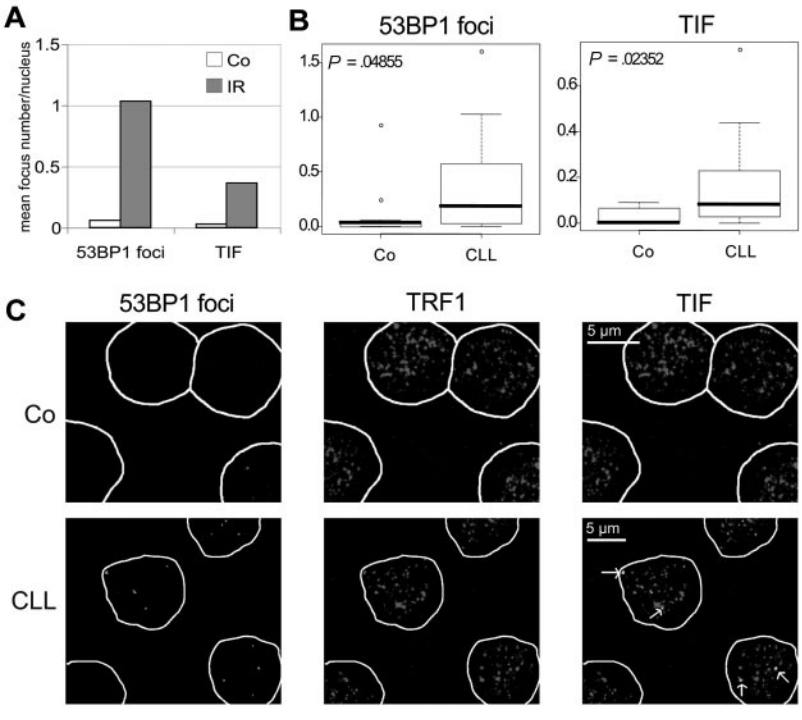

Figure 3. Telomeric damage induced foci in B cells from healthy donors and CLL patients. Confocal immunofluorescence analyses of 53BP1 foci and TRF1/53BP1 colocalization (TIF). (A) CLL B cells isolated from one CLL patient were subjected (IR) or no (Co) to 5 Gy γ-IR and fixed for immunostaining 1 hour latter. Median number of 53BP1 foci and TIF per nucleus is shown. (B-C) B cells from 11 healthy donors (Co) and 18 CLL patients (CLL) were immunostained for 53BP1 and TRF1; 53BP foci and TIF were scored after confocal analysis. (B) Box plot showing number of 53BP1 foci (left) and TIF (right) per nucleus; Wilcoxon-calculated *P* values are indicated in each box plot. (C) Immunofluorescence representing pictures of 53BP1 foci (left), TRF1 labeling (middle), and TIF (right) in B cells from healthy donor (top) and CLL patient (bottom). Arrows indicate TIF; TOTO staining is outlined in the equatorial plane of the nucleus. Detailed of ×60 magnification are shown after z-stack reconstruction (Image J software).

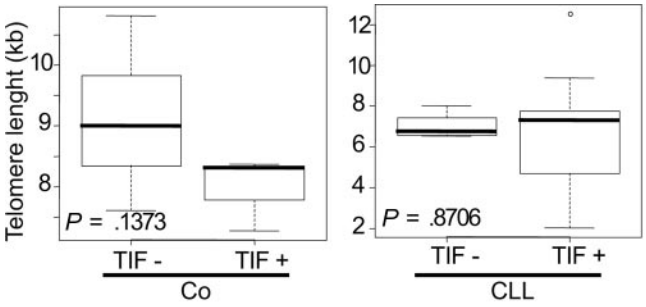

Figure 4. Telomere damages are not correlated with telomere shortening in CLL cells. Telomere restriction fragment analyzes were done on B lymphocytes purified from 12 healthy donors and 20 CLL patients. Box plot showing telomere size, with corresponding Wilcoxon test–calculated *P* values in cells bearing (TIF$^+$) or not (TIF$^-$) TIF among the healthy (Co, left) or the CLL panel (CLL, right).

telomeres tend to be shorter in the TIF$^+$ healthy subgroup, this is not the case in the TIF$^+$ CLL subgroup (Figure 4). We also used as a cutoff the maximal number of TIF observed in healthy donors, this segregated CLL patients into 2 equal groups (TIF low and TIF high). Even using this method we failed to observed a diminution in telomere size in the TIF-high subgroup (supplemental Figure 1, available on the *Blood* Web site; see the Supplemental Materials link at the top of the online article). Thus, if a shorter telomere length could be the principal cause of telomere dysfunction in normal B cells, it does not seem to be the case in CLL cells of stage A patients. This suggests that the appearance of TIF in early stages of the disease does not mainly result from replicative erosion but rather from altered capping functions. This does not exclude the possibility that some TIFs result from a complete or nearly complete deletion of telomeres as previously observed in more advanced stage.[12] In agreement with this view, whereas no clear correlation is found between telomere shortening and TIF increase when normal individuals are compared with stage A patients ($P = .1526$), the correlation is significant ($P = .0047$) comparing normal individuals to 4 cases of stage B and C patients (supplemental Figure 1).

Telomeric nucleosome status in CLL

Next, we wonder whether telomeric chromatin alterations could explain TIF formation in CLL cells. Thus, we performed ChIP experiments against histone modifications known to characterize "repressive" (H3 lysine 9 trimethylation: H3K9trim), or "active" chromatin (H3 lysine 9 acetylation: H3K9ac) and against total histone H3. We used an irrelevant IgG as a control and estimated telomeric versus Alu sequences enrichment in the immunoprecipitated fractions. We did not observe any significant alterations of the tested histone marks in CLL compared with normal samples, although we noted a trend toward an increased H3K9ac in CLL samples ($P = .0539$; Figure 5A-B). Interestingly, we also observed a propensity of the TIF$^+$ healthy subgroup toward an increased presence of the H3K9ac mark at telomeres while this trend is totally lost in the TIF$^+$ subgroups of CLL patients (Figure 5C). Although we failed to establish any statistically significant difference in the telomeric chromatin status of healthy versus CLL cells, our results are compatible with a common modification of chromatin state in CLL with a trend toward a more open conformation.

A decreased expression of *TINF2* and *ACD* correlates with TIF formation in CLL

Because loss or imbalance of shelterin components can induce TIF formation and because we previously reported a deregulation in shelterin gene expression in CLL, we asked whether TIF formation correlates with deregulation of shelterin expression in CLL cells. Therefore, we compared the mRNA expression levels of *TERF1*, *TERF2*, *TINF2*, *TERF2IP* (coding for RAP1), *POT1*, and *ACD* (coding for TPP1) between the TIF$^-$ and TIF$^+$ subgroup of CLL patients. There is a global tendency toward a down-regulation of shelterin component mRNA level in the TIF$^+$ CLL subgroup

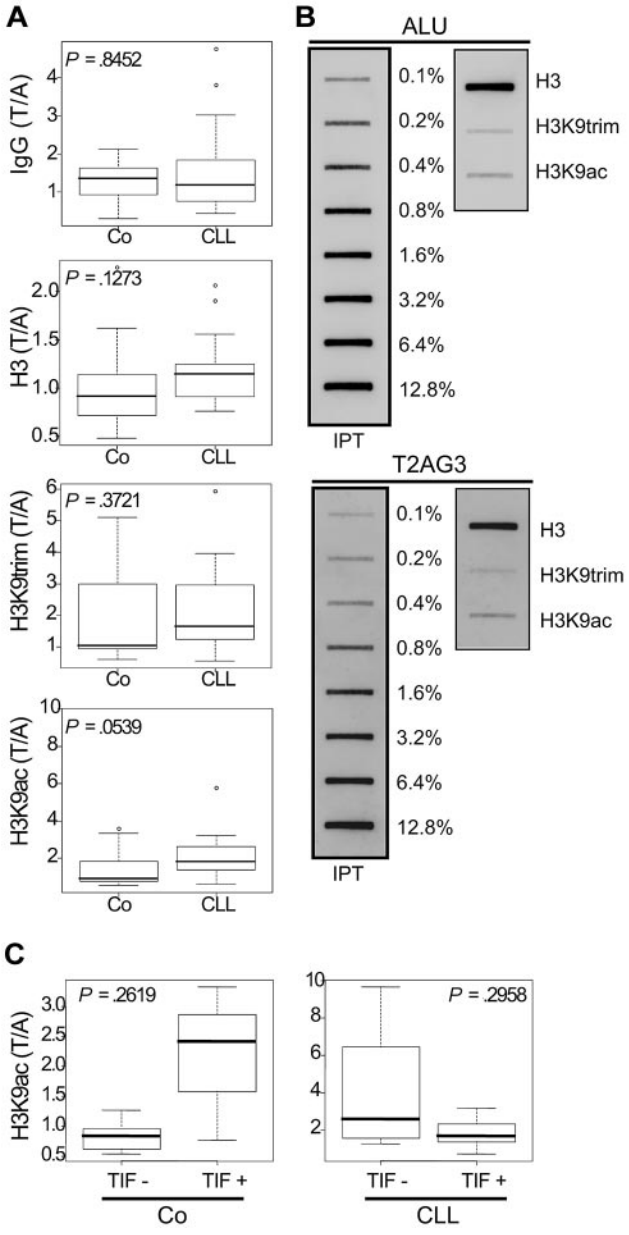

Figure 5. Telomeric histone modifications. (A-C) Immunoprecipitations against histone H3 (H3), trimethylated H3K9 (H3K9trim), and acetylated H3K9 (H3K9ac) were performed on chromatin isolated from B cells of 21 CLL patients and 12 healthy donors. An irrelevant IgG instead of specific antibodies was used in the control condition. Slot-blot analyses of telomeric and Alu sequences enrichment were performed using specific probes. Specific enrichment in immunoprecipitated fraction was estimated relatively to the INPUT fraction, and quantified thanks to a total input dilution range. (A,C) Box plots show relative enrichments of telomeric versus Alu sequences (T/A) for different immunoprecipitations. Corresponding Wilcoxon tests *P* values are inserted in box plots. (A) Comparison of ChIP realized on CLL B cells (CLL) versus normal B cells (Co) and (C) comparison of ChIP results obtained among normal (Co) or CLL (CLL) B cells bearing (TIF$^+$) or not (TIF$^-$). (B) Representative result of a ChIP experiment performed on B cells from a CLL patient, showing, on the left the input range (IPT) used for the quantification and on the right the dots obtained after deposit of 10% of total H3, H3K9trim and H3K9ac immunoprecipitates. The membrane was revealed using ALU (top) or telomeric probes (bottom).

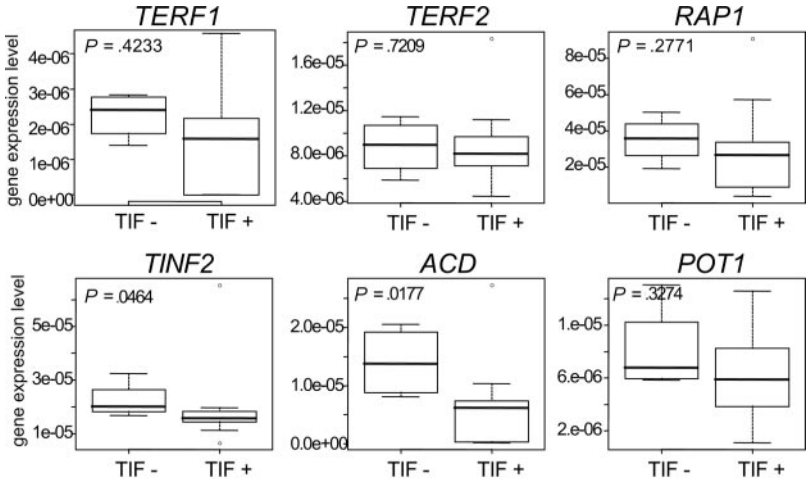

Figure 6. Shelterin component mRNA level in CLL B cells in function of TIF presence. Normalized genes expression level of *TERF1*, *TERF2*, *RAP1*, *TINF2*, *ACD*, and *POT1*. mRNA were extracted from purified B cells of 20 CLL patients demonstrating (TIF^+) or not (TIF^-) telomeric damages. Wilcoxon test calculated *P* values are indicated in each corresponding box plot.

(Figure 6). This is statistically significant for *TINF2* ($P = .0464$) and *ACD* ($P = .0177$). This suggests that telomere dysfunction in CLL cells could result from an aberrant expression of *TINF2* and *ACD*.

Discussion

We report here for the first time a telomere dysfunction in early stages of CLL. Interestingly, the presence of telomere DNA damage–induced foci (TIF) in CLL patients correlates with a reduced expression of the *ACD* and *TINF2* shelterin genes but not with short telomeres.

It was previously reported that telomere shortening because of cell proliferation (in the absence of telomerase) results in TIF accumulation associated with an increase in telomeric H3K9 acetylation.[37,38] In agreement with this scheme, we found that the presence of TIF in normal B cells tends to correlate with shorter telomeres and an increased presence of H3K9ac at telomere. However, there is no tendency toward telomere shortening in patients harboring a detectable level of TIF. Thus, the TIF increase in our cohort of stage A patients cannot be merely explained by telomere shortening because of cell overproliferation. In agreement with previous works showing an increased rate of proliferation[39] and telomere crisis[12] in advanced stage of CLL, we observed a significant correlation between the presence of TIF and short telomeres in patients at stages B and C. We therefore conclude that early stages of CLL is associated with telomere deprotection, which cannot be merely explained by telomere shortening, while advanced stages, probably as a consequence of an increased number of cell divisions, lead to critically short telomeres triggering DNA damage response and chromosome end fusion.

We noted a global decrease in the expression of shelterin component encoding genes in the stage A CLL patients harboring telomere damage and in particular a significant decrease in the expression of both *ACD* and *TINF2* genes. Considering the shelterin complex conformation, TRF1 and TRF2 bind the duplex telomeric DNA and POT1 the single-strand 3′ overhang. POT1 function as an heterodimer with TPP1 (encoded by *ACD*) which enhances its binding to telomeres.[12] TIN2 (encoded by *TINF2*) plays a major role in the complex stabilization, by bridging TPP1, TRF1, and TRF2.[40,41] Thus, both *ACD* and *TINF2* encode proteins playing a central role in the formation of the shelterin protein bridge linking the duplex part to the 3′ overhang of telomeric DNA. Their loss is thus expected to dissociate an essential capping structure.[40-43] Therefore, we propose that increased TIF occurrence in stage A CLL patients results, at least in part, from a partial disassembly of the shelterin complex.

What could be the role of damaged telomeres in CLL pathogenesis? Because the presence of TIF is a hallmark of senescent cells[36] and of senescent T lymphocytes in particular,[44] we propose that early stage CLL is associated to accelerated B-lymphocyte senescence. This might result from the accumulation of various telomere dysfunctions in the B-cell lineage, including telomerase and shelterin down-regulation ([8] and this work). In agreement with this view, CLL B cells are known to be initially G0 arrested[45] and we observed an increase in p16 expression in our cohort of CLL patients (Figure 2A). Escape from senescence induce telomere-excessive shortening, fusion, and cell-crisis entry and promote genome instability.[6] Increase in cell proliferation,[39] fused-telomere and crisis-like phenotype have very recently been reported in more advanced stage of CLL.[12] It could thus be possible that progression toward more advanced stage or transformation in the aggressive Richter syndrome are associated with senescence bypass.

To our knowledge, this work provides the first evidence of telomere deprotection in a human malignancy in link with an alteration of the shelterin complex. Interestingly, these damages occur at an early stage of the disease, suggesting that they contribute to the early step of malignant transformation. This enlightens the concept, well documented in mouse models but still hypothetical in human cancer, that telomere dysfunction facilitates cancer initiation.[6,46]

Acknowledgments

The authors thank G. Belz for help on statistical analyses.

This work was supported by grants from la Ligue Nationale contre le Cancer (équipe labelisée), ARECA program on Epigenetic Profiling, INCa (program TELINCA and TELOFUN), and the European Union (FP7-Telomarker, Health-F2-2007-200950).

Authorship

Contribution: A.A., C.T.d.R., T.S., S.B., B.H., and D.P. performed experiments; M.C., D.L., L.J., and G.S. collected biologic samples;

and E.G. and D.P. designed the research, analyzed the results, made the figures, and wrote the paper.

Conflict-of-interest disclosure: The authors declare no competing financial interests.

Correspondence: Eric Gilson, University of Nice, Laboratory of Biology and Pathology of Genomes, UMR 6267 CNRS U998 Inserm, 28 avenue Valombrose, Faculté de Médecine 06107 Nice Cedex 2, France; e-mail: eric.gilson@unice.fr.

References

1. Gilson E, Geli V. How telomeres are replicated. *Nat Rev Mol Cell Biol.* 2007;8(10):825-838.
2. Deng Y, Chan SS, Chang S. Telomere dysfunction and tumour suppression: the senescence connection. *Nat Rev Cancer.* 2008;8(6):450-458.
3. Greider CW, Blackburn EH. Identification of a specific telomere terminal transferase activity in tetrahymena extracts. *Cell.* 1985;43(2 Pt 1):405-413.
4. Kim NW, Piatyszek MA, Prowse KR, et al. Specific association of human telomerase activity with immortal cells and cancer. *Science.* 1994; 266(5193):2011-2015.
5. Brunori M, Luciano P, Gilson E, Geli V. The telomerase cycle: normal and pathological aspects. *J Mol Med.* 2005;83(4):244-257.
6. Artandi SE, Chang S, Lee SL, et al. Telomere dysfunction promotes non-reciprocal translocations and epithelial cancers in mice. *Nature.* 2000;406(6796):641-645.
7. Rossi D, Lobetti Bodoni C, Genuardi E, et al. Telomere length is an independent predictor of survival, treatment requirement and Richter's syndrome transformation in chronic lymphocytic leukemia. *Leukemia.* 2009;23(6):1062-1072.
8. Poncet D, Belleville A, t'kint de Roodenbeke C, et al. Changes in the expression of telomere maintenance genes suggest global telomere dysfunction in B-chronic lymphocytic leukemia. *Blood.* 2008;111(4):2388-2391.
9. Jahrsdorfer B, Weiner GJ. Short telomeres in B-CLL: the chicken or the egg? *Blood.* 111(12): 5756, 2008; author reply 5756-5757.
10. Ricca I, Rocci A, Drandi D, et al. Telomere length identifies two different prognostic subgroups among VH-unmutated B-cell chronic lymphocytic leukemia patients. *Leukemia.* 2007;21(4):697-705.
11. Brugat T, Nguyen-Khac F, Grelier A, Merle-Beral H, Delic J. Telomere dysfunction-induced foci arise with the onset of telomeric deletions and complex chromosomal aberrations in resistant chronic lymphocytic leukemia cells. *Blood.* 2010;116(2): 239-249.
12. Lin TT, Letsolo BT, Jones RE, et al. Telomere dysfunction and fusion during the progression of chronic lymphocytic leukemia: evidence for a telomere crisis. *Blood.* 2010;116(11):1899-1907.
13. Blackburn EH, Greider CW, Szostak JW. Telomeres and telomerase: the path from maize, tetrahymena and yeast to human cancer and aging. *Nat Med.* 2006;12(10):1133-1138.
14. de Lange T. Shelterin: the protein complex that shapes and safeguards human telomeres. *Genes Dev.* 2005;19(18):2100-2110.
15. Palm W, de Lange T. How shelterin protects mammalian telomeres. *Annu Rev Genet.* 2008; 42:301-334.
16. Lei M, Zaug AJ, Podell ER, Cech TR. Switching human telomerase on and off with hPOT1 protein in vitro. *J Biol Chem.* 2005;280(21):20449-20456.
17. Loayza D, De Lange T. POT1 as a terminal transducer of TRF1 telomere length control. *Nature.* 2003;423(6943):1013-1018.
18. van Steensel B, de Lange T. Control of telomere length by the human telomeric protein TRF1. *Nature.* 1997;385(6618):740-743.
19. Wang F, Podell ER, Zaug AJ, et al. The POT1-TPP1 telomere complex is a telomerase processivity factor. *Nature.* 2007;445(7127):506-510.
20. Jiang WQ, Zhong ZH, Henson JD, Reddel RR. Identification of candidate alternative lengthening of telomeres genes by methionine restriction and RNA interference. *Oncogene.* 2007;26(32):4635-4647.
21. Nakanishi K, Kawai T, Kumaki F, et al. Expression of mRNAs for telomeric repeat binding factor (TRF)-1 and TRF2 in atypical adenomatous hyperplasia and adenocarcinoma of the lung. *Clin Cancer Res.* 2003;9(3):1105-1111.
22. Blanco R, Munoz P, Flores JM, Klatt P, Blasco MA. Telomerase abrogation dramatically accelerates TRF2-induced epithelial carcinogenesis. *Genes Dev.* 2007;21(2):206-220.
23. Biroccio A, Rizzo A, Elli R, et al. TRF2 inhibition triggers apoptosis and reduces tumourigenicity of human melanoma cells. *Eur J Cancer.* 2006; 42(12):1881-1888.
24. Blasco MA. The epigenetic regulation of mammalian telomeres. *Nat Rev Genet.* 2007;8(4):299-309.
25. Garcia-Cao M, O'Sullivan R, Peters AH, Jenuwein T, Blasco MA. Epigenetic regulation of telomere length in mammalian cells by the Suv39h1 and Suv39h2 histone methyltransferases. *Nat Genet.* 2004;36(1):94-99.
26. Benetti R, Gonzalo S, Jaco I, et al. Suv4-20h deficiency results in telomere elongation and derepression of telomere recombination. *J Cell Biol.* 2007;178(6):925-936.
27. Gonzalo S, Jaco I, Fraga MF, et al. DNA methyltransferases control telomere length and telomere recombination in mammalian cells. *Nat Cell Biol.* 2006;8(4):416-424.
28. Mehes G. Chromosome abnormalities with prognostic impact in B-cell chronic lymphocytic leukemia. *Pathol Oncol Res.* 2005;11(4):205-210.
29. Matthews C, Catherwood MA, Morris TC, et al. Serum TK levels in CLL identify Binet stage A patients within biologically defined prognostic subgroups most likely to undergo disease progression. *Eur J Haematol.* 2006;77(4):309-317.
30. Rossi D, Sozzi E, Puma A, et al. The prognosis of clinical monoclonal B cell lymphocytosis differs from prognosis of Rai 0 chronic lymphocytic leukaemia and is recapitulated by biological risk factors. *Br J Haematol.* 2009;146(1):64-75.
31. Hanada M, Delia D, Aiello A, Stadtmauer E, Reed JC. bcl-2 gene hypomethylation and high-level expression in B-cell chronic lymphocytic leukemia. *Blood.* 1993;82(6):1820-1828.
32. Klein U, Tu Y, Stolovitzky GA, et al. Gene expression profiling of B cell chronic lymphocytic leukemia reveals a homogeneous phenotype related to memory B cells. *J Exp Med.* 2001;194(11):1625-1638.
33. Bechter OE, Eisterer W, Pall G, Hilbe W, Kuhr T, Thaler J. Telomere length and telomerase activity predict survival in patients with B cell chronic lymphocytic leukemia. *Cancer Res.* 1998;58(21): 4918-4922.
34. Grabowski P, Hultdin M, Karlsson K, et al. Telomere length as a prognostic parameter in chronic lymphocytic leukemia with special reference to VH gene mutation status. *Blood.* 2005;105(12): 4807-4812.
35. Roos G, Krober A, Grabowski P, et al. Short telomeres are associated with genetic complexity, high-risk genomic aberrations, and short survival in chronic lymphocytic leukemia. *Blood.* 2008; 111(4):2246-2252.
36. Takai H, Smogorzewska A, de Lange T. DNA damage foci at dysfunctional telomeres. *Curr Biol.* 2003;13(17):1549-1556.
37. d'Adda di Fagagna F, Reaper PM, Clay-Farrace L, et al. A DNA damage checkpoint response in telomere-initiated senescence. *Nature.* 2003;426(6963): 194-198.
38. Benetti R, Garcia-Cao M, Blasco MA. Telomere length regulates the epigenetic status of mammalian telomeres and subtelomeres. *Nat Genet.* 2007;39(2):243-250.
39. Messmer BT, Messmer D, Allen SL, et al. In vivo measurements document the dynamic cellular kinetics of chronic lymphocytic leukemia B cells. *J Clin Invest.* 2005;115(3):755-764.
40. Ye JZ, Donigian JR, van Overbeek M, et al. TIN2 binds TRF1 and TRF2 simultaneously and stabilizes the TRF2 complex on telomeres. *J Biol Chem.* 2004;279(45):47264-47271.
41. O'Connor MS, Safari A, Xin H, Liu D, Songyang Z. A critical role for TPP1 and TIN2 interaction in high-order telomeric complex assembly. *Proc Natl Acad Sci U S A.* 2006;103(32):11874-11879.
42. Kim SH, Beausejour C, Davalos AR, Kaminker P, Heo SJ, Campisi J. TIN2 mediates functions of TRF2 at human telomeres. *J Biol Chem.* 2004; 279(42):43799-43804.
43. Tejera AM, Stagno d'Alcontres M, Thanasoula M, et al. TPP1 is required for TERT recruitment, telomere elongation during nuclear reprogramming, and normal skin development in mice. *Dev Cell.* 2010;18(5):775-789.
44. Chebel A, Bauwens S, Gerland LM, et al. Telomere uncapping during in vitro T-lymphocyte senescence. *Aging Cell.* 2009;8(1):52-64.
45. Zenz T, Mertens D, Kuppers R, Dohner H, Stilgenbauer S. From pathogenesis to treatment of chronic lymphocytic leukaemia. *Nat Rev Cancer.* 2010;10(1):37-50.
46. Rudolph KL, Millard M, Bosenberg MW, DePinho RA. Telomere dysfunction and evolution of intestinal carcinoma in mice and humans. *Nat Genet.* 2001;28(2):155-159.

2011 118: 1316-1322
doi:10.1182/blood-2010-07-295774 originally published online February 25, 2011

Telomeric damage in early stage of chronic lymphocytic leukemia correlates with shelterin dysregulation

Adeline Augereau, Claire T'kint de Roodenbeke, Thomas Simonet, Serge Bauwens, Béatrice Horard, Mary Callanan, Dominique Leroux, Laurent Jallades, Gilles Salles, Eric Gilson and Delphine Poncet

Blood (print ISSN 0006-4971, online ISSN 1528-0020), is published weekly by the American Society of Hematology, 2021 L St, NW, Suite 900, Washington DC 20036.